SZENT ISTVÁN EGYETEM

THESIS OF (PhD) DISSERTATION

Modelling of gaseous diffusion in undisturbed soil samples in function of soil structure

Gyarmati Bernadett

Gödöllő

2013

Szent István University - Doctoral School

Name: **Doctoral School of Environmental Sciences**

Discipline: **Environmental Sciences**

Head: **Dr. György Heltai DSc.**

Szent István University,
Faculty of Agricultural and Environmental Sciences
Institute of Environmental Sciences
Department of Chemistry and Biochemistry

Supervisors: **Dr. Ágnes Ilona Mészárosné Bálint PhD**

Szent István University,
Faculty of Agricultural and Environmental Sciences
Institute of Environmental Sciences
Department of Chemistry and Biochemistry

Dr. Csaba Mészáros PhD

Szent István University
Faculty of Mechanical Engineering
Department of Physics and Process Control

……

Head of School's approval

……

……

Supervisors' approvals

BACKGROUND AND OBJECTIVES

Transport processes in the Earth's crust are very diverse. Crude oil exploration, processes of applying artificial fertilizers or organic manures are closely related to this topic. Without knowing the condition of the fertile upper layer of Earth's crust it is difficult to answer successfully questions concerning complex energetic, agricultural and/or environmental challenges. Experimental and theoretic examination and computer simulation of transport processes in porous medium are crucial parts of revealing mass and energy flows occurring at the soil-atmosphere interface and under the surface. It is a completely open research area with several questions unanswered and with the possibility of developing and applying new modelling methods.
In my present work I selected an environmentally important topic from the transport problems: I examined the gaseous diffusion in undisturbed soil samples in function of soil structure properties.

- First step as well as the first goal was the generation of adequate database for the further examination. In order to collect data I used my own designed experimental setup, which was compatible with the experimental setup built for theoretical (Mészáros et al. 2011, Kirschner et al. 2007) and experimental (Nagy et al. 2011) examination of convection. The system was also compatible with the multistep outflow system (MSO) designed to measure the soil hydraulic conductivity and retention (Weller et al. 2011).

  In the first part of my work, I collected eight soil monoliths with different texture, 350 mm in height and 180 mm in diameter. After determination of the general soil properties, sterilization and sample preparation, they were connected to the (MSO compatible) gas diffusion experimental system with continuous gas supply. Thus the emission and changes of CO_2, N_2O, CH_4 gas concentration were followed during ten day long experiments. Due to the experimental results the relative gas diffusion coefficients were determined for each gas. Afterwards samples were scanned in high resolution by computed tomography (CT).

After the experimental part my aims were the followings:

- In this work segmentation of the CT images is the critical step, which is also true in medical data processing. There is a strict, standardized protocol for image segmentation in medical

practice which does not exist in case of geological samples. Thus I chose examination of three segmentation methods recommended for soil samples in the relevant literature (wherein the applied threshold by binarization were Th_1, Th_2, and Th_3).

- By the help of advanced image processing software and based on the segmented CT data matrix, my further objects were the soil macropore space visualization and comprehensive pore space characterization. Characterisation of the soil structure covered the following properties: macroporosity, effective porosity, average macropore size and diameter, total surface area, macroporous network density, tortuosity, node density, and pore space skeleton. Most of the experiments designed for examining gaseous diffusion use undisturbed samples with volume 200 cm^3 or less, which are not suitable to represent the heterogeneity of nature soils, thus it gives significance of this research task. Therefore, database originating from three-dimensional reconstruction of soil monoliths are particular valuable.

- Another goal was to analyse the relationship between the soil characteristics properties based on three-dimensional computer tomography reconstruction and the relative diffusion coefficient derived from the gas diffusion experiment. However, I would like to emphasize that this type of experimental combination is very rare, so this task includes only the elaboration and presentation of a new analyses possibility. Therefore, this objective excludes the presentation and analysis of soil transport properties in function of soil structure characteristic based on genetic soil classification (which is far beyond available budget of a doctoral research).

  The implementation of the study trying to open new approaches since computer tomographic studies mainly focus on fluid phase transport (hydraulic conductivity).

- Estimation on relative soil gas diffusion coefficient becomes more and more important because of greenhouse gas emissions originating from the soil and contributing to global climate change. Therefore it is very important to outline those soil properties (based on CT database) which have significant relationship with soil gaseous diffusivity. In addition, I would like to test the well-known, one and two parameter models predicting relative gaseous diffusion coefficient with CT input data from the three different segmentation techniques.

MATERIAL AND METHODS

Soil sampling:

I collected eight intact soil monoliths with different texture, 350 mm in height and 180 mm in diameter by the help of a special soil sample holder (DIN EN ISO 15493). The reason behind the non-standardised sampling method was to maintain the compatibility with other experimental system (MSO, multi-step-outflow (Weller et al., 2011); soil convection (Nagy et al., 2011). By sampling primary objective was to preserve the original structure.

In addition, small samples (350 mm in height and 100 mm in diameter) were also collected just next to the soil monoliths in order to perform collateral examinations (particle size distribution, bulk density, organic content etc.).

Table 1. contains the data on sampling (sampling location, depth) with the results of the collateral examination, wherein labels (capital letters) DU-T, EL-T, ID-T, KI-T, KO-T, LA-T, LI-T. MO-T belongs to the undisturbed samples, while small samples were marked with small letter analogously.

Sample preparation:

-Soil sterilization:

Gamma radiation was used (30 kGy) (Izotóp Intézet Kft.) to eliminate post sampling structural modification caused by soil flora and fauna and inhibits soil microbiological gas production.

-Adjusting the soil moisture content:

At first, full saturation was reached by wetting the samples gently based on the hydrostatic law of communicating vessels. Subsequently they were drained to -200 cm water potential (-19,6 kPa pressure potential) (hanging water column) by the help of sterilized column 2500 mm in height and 400 mm in diameter, thus assumption of being approximately at field capacity could be drawn.

Collateral examinations:

-Bulk density, soil organic matter and particle size distribution:

Bulk density was determined according to Blake and Hartke (1986). SEDIMAT 4-12 (Umwelt-Geräte-Technik GmbH, Müncheberg, Germany) laboratory apparatus was used for determination of particle size distribution in soil material with 4 fractions by DIN ISO 11277. Wet sifting was done to complete the partitioning beyond 0.063 mm. Hydrogen peroxide digestion method was used for organic matter determination described in detail by Schumacher (2002).

Table 1.: Sampling data and results of the collateral examinations

Sample ID	Subsample ID	Sampling place	Sampling depth (mm)	Bulk density	Particle size density*	Organic matter (%)	Particle sizedistribution (%) Clay	Fine silt	Medium silt	Coarse silt	Fine sand	Medium sand	Coarse sand	Error (%)
DU-T		N 47° 26' E 19° 28'	0-350											
	Du-a		250-350	1,53	2,43	4,5	23,34	4,44	13,54	30,24	19,91	2,52	3,26	2,75
	Du-b		150-250	1,50	2,65	2,4	24,74	2,16	9,38	29,77	29,59	1,20	0,57	2,59
	Du-c		50-150	1,49	2,48	3,6	33,59	8,19	9,85	22,26	20,53	1,62	0,56	3,39
	Du-d		0-50	1,46	2,57	3,6	25,94	6,71	6,91	20,56	24,52	12,29	1,03	2,04
EL-T		N 47° 31' E 19° 22'	0-350											
	EL-a		250-350	1,45	2,52	2,2	15,10	2,53	11,29	36,76	29,82	1,13	0,94	2,44
	El-b		150-250	1,46	2,51	3,3	19,21	1,87	11,52	38,87	22,50	1,08	1,59	3,37
	EL-c		50-150	1,46	2,52	4	19,14	9,37	3,13	39,39	23,23	2,14	0,63	2,97
	El-d		0-50	1,40	2,56	1,8	23,11	2,23	9,63	27,97	28,45	4,59	1,82	2,19
ID-T		N 51° 24' E 11° 53'	0-350											
	Id-a		250-350	1,54	2,52	4,5	25,67	5,53	20,55	42,61	2,75	0,88	0,33	1,67
	Id-b		150-250	1,52	2,42	3,8	26,47	3,75	20,38	39,25	5,41	2,16	0,65	1,93
	Id-c		50-150	1,48	2,38	4,3	32,17	5,98	17,58	32,35	7,11	1,97	0,66	2,18
	Id-d		0-50	1,48	2,42	6	28,76	2,51	4,92	48,46	9,48	2,31	0,66	2,90
KI-T		N 51° 31' E 11° 51'	20-370											
	Ki-a		270-370	1,28	2,26	4,6	19,36	2,12	8,16	10,88	31,64	21,83	4,74	1,27
	Ki-b		170-270	1,31	2,32	3,7	25,76	3,54	10,51	13,65	19,78	21,41	3,57	1,77
	Ki-c		70-170	1,37	2,25	4,1	11,16	1,75	36,87	0,39	19,09	23,46	4,47	2,81
	Ki-d		20-70	1,31	2,35	7,2	27,45	0,52	12,15	14,66	16,54	20,95	4,30	3,43
KO-T		N 51° 32' E 11° 48'	0-350											
	Ko-a		250-350	1,37	2,29	3	18,53	8,65	5,87	1,13	17,79	41,56	2,88	3,60
	Ko-b		150-250	1,36	2,49	4,7	21,70	2,23	4,02	7,95	18,58	39,04	2,99	3,48
	Ko-c		50-150	1,35	1,19	6,4	27,82	3,42	2,38	5,36	16,32	37,93	2,76	4,02
	Ko-d		0-50	1,41	1,01	9,2	23,89	6,80	3,66	13,42	19,29	25,57	2,66	4,71
LA-T		N 47° 33' E 18° 56'	20-370											
	La-a		270-370	1,44	2,34	4,2	43,44	10,47	9,99	8,07	19,16	2,43	3,16	3,27
	La-b		170-270	1,44	2,44	4,6	37,08	11,42	11,95	4,69	30,16	1,23	0,59	2,88
	La-c		70-170	1,54	2,38	4,8	27,75	7,45	13,84	25,96	20,89	1,61	0,56	1,93
	La-d		20-70	1,44	2,39	4,4	32,53	9,84	14,43	4,67	23,97	11,73	0,98	1,85
LI-T		N 51° 22' E 11° 57'	10-360											
	Li-a		260-360	1,54	2,40	3,5	28,77	8,31	13,37	17,38	18,62	9,58	2,05	1,93
	Li-b		160-260	1,49	2,32	3,7	20,71	4,25	11,18	13,91	24,84	14,58	9,29	1,26
	Li-c		60-160	1,60	2,35	3,3	21,46	3,56	27,78	21,59	12,41	8,99	1,82	2,39
	Li-d		10-60	1,50	2,49	3,8	35,75	10,17	16,91	5,76	25,19	0,11	2,91	3,21
MO-T		N 47° 27' E 19° 21'	0-350											
	Mo-a		250-350	1,49	2,59	2,3	18,86	1,52	7,22	11,81	27,87	28,98	0,95	2,78
	Mo-b		150-250	1,45	2,60	1,8	12,01	0,60	3,98	7,50	27,10	45,38	1,45	1,97
	Mo-c		50-150	1,49	2,58	3,2	18,30	6,15	6,13	8,31	27,36	30,37	0,44	2,94
	Mo-d		0-50	1,48	2,61	1,7	20,75	4,20	4,29	8,83	27,09	26,09	6,28	2,48

* determined by pycnometer

Description of the diffusion experiment:

-Sample preparation for the diffusion experiment:

After adjusting the soil water content, samples were fixed with silicone adhesive (Ceresit Sanitär Silikon) into a plastic plate to ensure gastight connection in the entire system. 3x5 sampling ports (cut glass vials, original headspace 20 ml, WIC 43220, WICOM, Germany**)**, capped with WICOM

Figure 1.: Sample preparation

20 mm butylrubber-septums, WIC 43699, WICOM Germany) with 120 degree shift were installed into the sides of columns at height of 80, 160, 240, 300 mm and at the top of the samples (gas sampling ports were labelled by analogy A-80 mm, B-160 mm, C-240 mm, D-300 mm, E-top). See Fig.1.

- Description of gas diffusion experimental setup:

Table 2.: Standard gas reservoir (DIN ISO 6141, Linde, 273,15 K; 101325 Pa)

NAME	NOMINAL VALUE ($cm^3\ m^{-3}$)	REAL VALUE ($cm^3\ m^{-3}$)	UNCERTANITY REL. (%)
CH_4	0,35	0,36	± 10
N_2O	18,0	17,0	± 2
CO_2	4,50	4,511	± 2
He	rest	rest	

Gas reservoir (Table 2.) with CH_4, N_2O, CO_2 gases, with reductor and digital flow meter apparatus, was attached to the bottom of the plastic base plate to supply the correct quantity of diffusing gas (10000 $cm^3\ day^{-1}$).

During the 10 day long investigation period, atmospheric pressure was measured by manometer and the temperature changed from 22.5 ± 1.5 °C. Gas samples (2 cm^3 gas with SGE 10 cm^3 Gas Tight and Dispenser Syringe) were taken from sampling ports in every four hours at the first two days and every 6 hours for the rest of the examination time. In order to determine the boundary conditions extra samples were taken each time in the air ("AIR"), about 400 mm above the top of the column and from the gas conducting pipe ("PIPE"), about 400 mm before the bottom joint on the plastic base. Gas samples were injected into glass vials (20 cm^3 headspace, WIC 43220, WICOM, Germany) pre-cleaned with He and measured by Shimadzu gas chromatograph (GC) GC-14 B PsF P/N 221-41665-34 (FID/ECD, Shimadzu Corp.) with Headspace Auto Sampler.

Processing of gas diffusion data:

Regarding the process of gas diffusion, the following assumptions were made: the direction of macroscopic diffusion is one-dimensional, it is parallel to axis z, which is the main axis of the soil column, advection and convection are negligible, so diffusion is the only dynamic process governing gas movement, adsorption and desorption are negligible (Liu et al. 2006).

By data processing of the gas measurements we relied on the quantitative description of Fick's law of diffusion:

$$j = -D_g \nabla C\,, \tag{1}$$

where j (kg m^{-2} s^{-1}) is the mass flux per unit area, D (m^2 s^{-1}) is the diffusion coefficient in general, C (kg m^{-3}) is the concentration. Combining Eq. [3] with the law of mass conservation

— , (2)

yields:

— , (3)

assuming that the diffusion coefficient D to be a constant in t time (s) and independent from temperature, pressure or concentration.

-Initial steps of data processing by Matlab (Version 7.12.0.635 (R2011a), MathWorks Inc.) required to apply numeric modelling approach according to Eq. (3).:

- The measured data from X, Y, Z directions were averaged at each soil depth (A, B, C, D, E). Data from "AIR", "PIPE" were used later for determining boundary conditions.
- Grid calculation: by the reason of unequally sampling in space and time, resampling of boundary and initial condition data was necessary to provide a calculation grid which is equally spaced and fine enough. Therefore, linear interpolation was applied to resample boundary conditions with 2 h steps equally form 0 h to 284 h in time and initial condition with 10 mm steps equally from -350 mm to 0 mm. By this way a computing grid resulted nodes (143 nodes in time and 36 nodes in space) (4. equation).

$$\left(\frac{284}{2}+1\right)\left(\frac{350}{2}+1\right)=5148 \tag{4}$$

-Solution and error calculation:

- Eq. (3) was solved by Matlab (MathWorks-ref1) which is an implicit finite difference method implementation for PDEs with maximum one dimension in space.
- After solving Eq.(3) it was possible to define an error metrics between model results and the measured gas concentration values, namely the squared sum of errors according to the following expression:

$$SSE=\sum_{i=1}^{n}(C_n-C_{Mn})^2 , \tag{5}$$

where n is the number of measured and processed concentration values, C_n denotes the n^{th} measured and processed concentration value, C_{Mn} is the nearest model result (in space and time) to C_n (Deza és Deza, 2009). Since parameter D_g is constant in time, it was possible to iterate with its value until the squared sum of error reached the minimum value. In this case,

this iteration was an optimum search problem and performed by a direct simplex search algorithm implementation of Matlab (MathWorks-ref2).

- The following error metrics was applied additionally to determine the error of the numerical model fitting (where all notations are the same as the previous error metric expression):

$$Err_A = \sum_{i=1}^{n} \frac{|C_n - C_{Mn}|}{|C_n|} 100 \quad . \tag{6}$$

Computed tomography scanning:

Computed tomography scanning took place two times because of the accurate estimation on effective porosity (air filled volume) and total porosity. Its necessity based on the drawback of the CT images, wherein voxels filled with the mixture of water and soil can not to be differentiated unambiguously. The first preparation was performed after the gas diffusion experiment, so soil samples held different amounts of water depending on their texture and structure. In order to reduce the effect of the different moisture level on the X-ray attenuation, all soil samples were re-wetted and drained with the same procedure, described above, thereby moisture content was approximately the same as at the beginning of the gas measurement.

Before the second CT measurement samples have been left to dry for a year whereby kind of soil condition was created wherein the assumption of total porosity is equal to the effective porosity is permissible. Therefore later comparison of CT images allowed the estimation of the amount of permeable volume blocked by presence of water.

CT scans were performed using a Siemens Somatom Sensation 16 Cardiac CT scanner (SIEMENS AG, Erlangen, Germany), and samples were imaged at 120 kV 250 mA, 1000 ms exposure to obtain the separation of different phases. The collected raw data were reconstructed by Somatom Syngo CT 2007S software. The resulted 16-bit, gray-scale images, with dimensions of 512 x 512 pixels, were used to create 3D imagery with a resolution of 0.391 x 0.391 x 1.20 mm^3 for each voxel size.

Intensity of the voxels was given in Hounsfield unit (HU), which is a density proportional unit and refers to the linear attenuation of X-ray beam in a given volume element.

Processing of CT data:

The aim of data processing was to identify and reconstruct macropore volumes inside the voxel matrix which contributed to create a permeable pathway in which gas diffusion has taken place. It required several steps, such as image cutting, threshold determination, resampling and filtering, segmentation, 3D reconstruction and quantification of several 3D attributes of the extracted networks.

-Image cutting:

Raw images were studied to identify the region of interest. By using Matlab software (Version 7.12.0.635 (R2011a), MathWorks Inc.) all dicom files were modified by replacing the measured HU values of voxels referring to the outside area of the soil column for an extreme high HU value, whereby disinterested void voxels will be excluded automatically by latter segmentation and resultant voxel intensity distribution remained the same in the range of void and solid matrix.

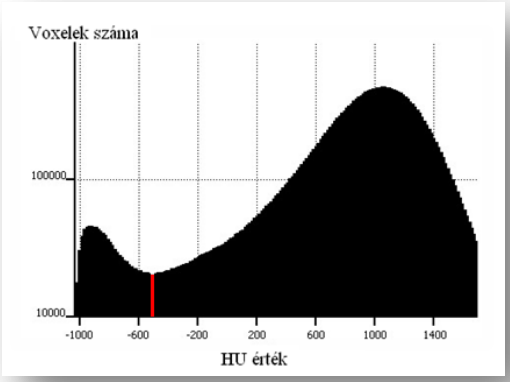

Figure 2.: Relevant histogram part of sample EL-T; voxels are presented in function of their HU value; Avizo Fire evaluation version 7.0.

-Threshold determination:

Determination of the threshold value was based on the greyscale histogram (accordingly on the HU values and their frequency distribution, see figure 2.). The major peak with the lowest mean HU number was assumed to correspond to the void space (air) and the next major peak was associated with solid material (water, soil and organic compound). The third, artificial peak consists of the voxels standing for the disregarded outside area.

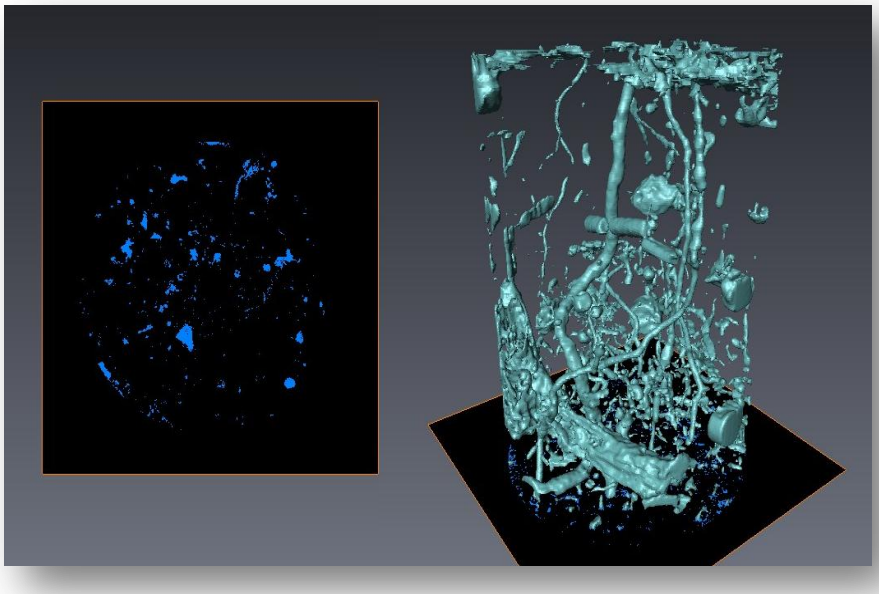

Figure 3.: Binarisation process with very low threshold value (-700 HU) by sample EL-T and the 3D reconstruction of the pore space network system

Three threshold values were tested in this work:

Th_1: was determined by finding the minimum value between the two major peaks, which is the so-called equi-probability point and commonly used threshold value in soil science (Tarquis et al., 2008). See figure 2. for sample EL-T.

Th_2: was determined based on the distance between the two major peaks (r), wherein Th_2 was equal to r/2.

Th_3: was determined according to Capowiez et al. (1998), where Th_3: was defined as r*2/3.

-Isotropic voxel (Avizo Fire, evaluation version 7.0.0., VSG-Visualization Sciences Group, SAS):

Hereinafter Avizo Fire (evaluation version 7.0.0., VSG-Visualization Sciences Group, SAS) was used to execute further data processing.

Initial anisotropic voxels (0.391 x 0.391 x 1.20 mm^3) were transformed into cubic voxels (0.45 x 0.45 x 0.45 mm^3) by sinc function based Lanczos algorithm (Meijering et al., 1999; Luo et al., 2010) in order to reduce morphological computational complexity.

-Noise reduction:

The Median filter, which is a very widely used nonlinear digital filtering technique, was applied to diminish noise and preserving edges.

-Segmentation:

Afterwards thresholding operation was done by segmenting voxels based on their intensity level until it reached the prior calculated threshold value (Th_1; Th_2; Th_3). It included also a binarization process, thus new binary field was created, wherein 1 is for each value within the threshold interval and 0 for all other field values. The results of the procedure can be seen on Figure 3.

-Labelling algorithm:

In this created binary field every separated macropore (object) was labelled and analysed by extracting numerical and statistical information individually for each object and summarised values for the entire column (number of macropores, macroporosity, mean pore size, surface area, network density).

-Skeletonisation:

Based on Sato et al. (2000)'s ''centerlinetree'' algorithm soil pores space skeleton can be created (see figure 4.). This algorithm contains a recursive erosion procedure. At first it defines a circle in every pore with the biggest radius in every given plane, and then starts to remove the voxels along the boundaries until removing the last voxel would eliminate the pore on the plane. Thus connecting the remaining voxels gives the centreline of a pore system, wherein voxels having connection with

more than 2 voxels are nodes (labelled with red points in Figure 4.). Nodes represent the connectivity of the soil pore space. Because of morphological complexity this procedure was done only in case of Th_1 and Th_2.

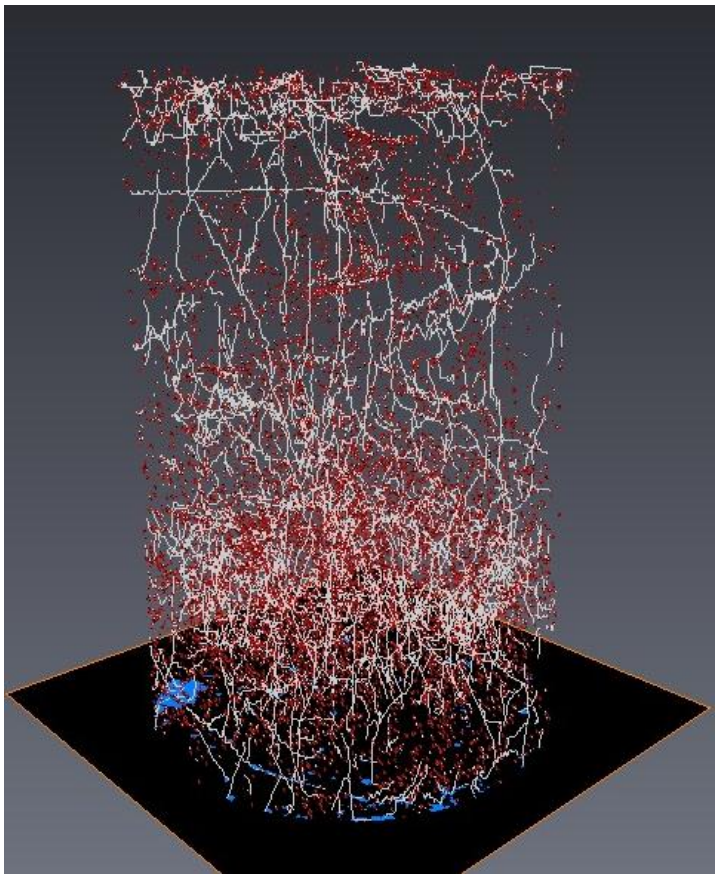

Figure 4.: Soil pore structure skeleton of sample EL-T

Generating soil pore space skeleton might have important role in case of dead pore space modelling.

RESULTS AND DISCUSSION

Analyses of the soil macropore system:

The different consistence of soil samples reflects on the visualisation of macropore network systems (Fig. 5).

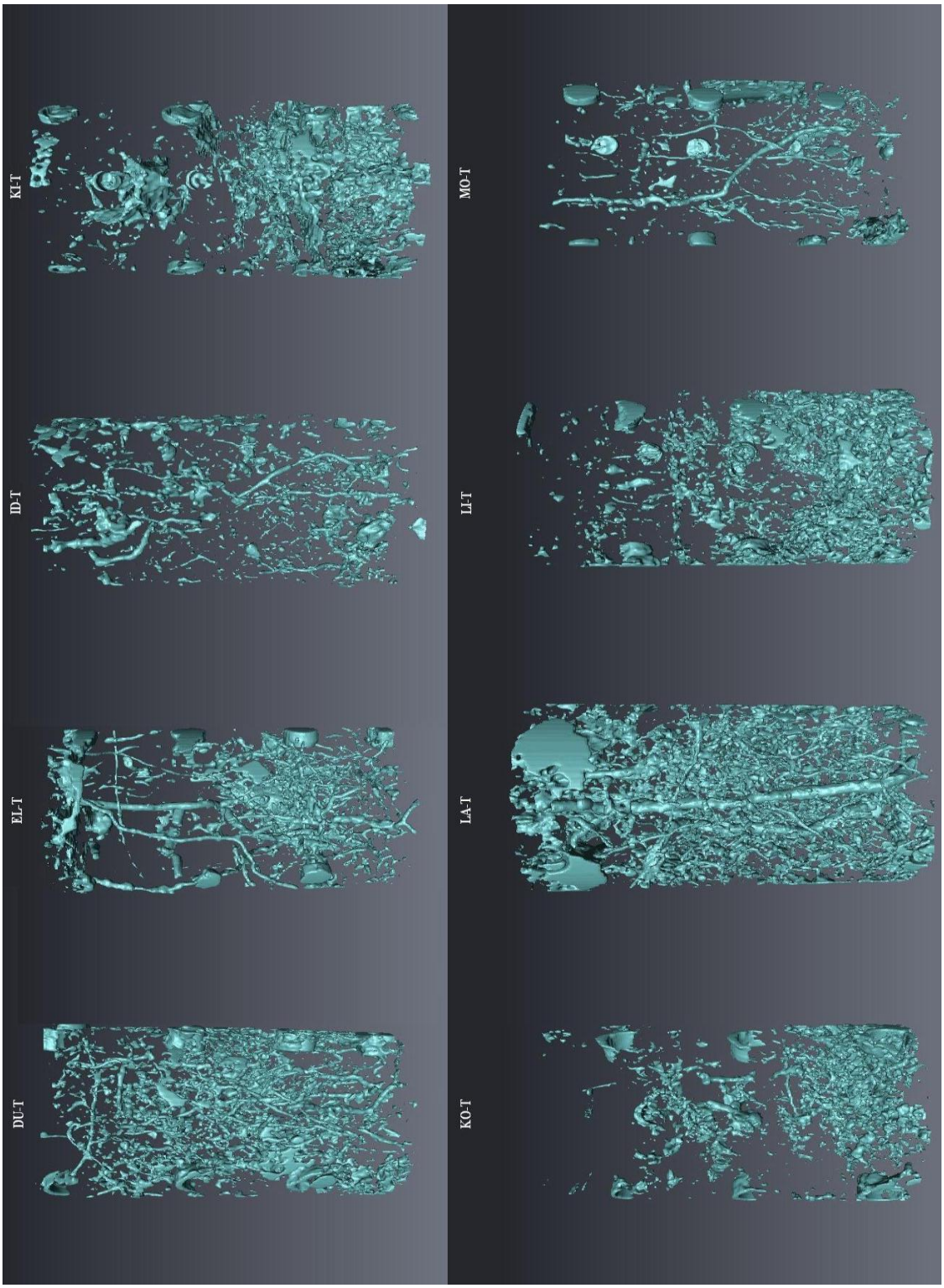

Figure 5.: 3D representation of the soil pore structure for each sample (DU-T, EL-T, ID-T, KI-T, KO-T, LA-T, LI-T, MO-T)

It can be stated, that highly continuous, relatively large and cylindrical macropores formed by either earthworms (*Lumbricidae)* or roots are occasionally broken (Fig.5-ID-T), which might originate from disturbance caused either during the transport, preparation or measurements or the inadequate operation of threshold value. The pore space can also be formed by freezing and melting the upper layer of the soil, which might generate irregular pore forms (Luo et al., 2010).

Since the resolution of our CT measurement already restricted the sensibility of fine pore system determination thus direct influences of small pore networks are disregarded.

Table 3.: Results of the CT examination in fuction of the three thresholds

	SAMPLE	TH VALUE	DETECTED	Macropor$_1$	Macropor$_2$	Average p. size	Area	Netw. Dens.	POM	α	Nodes	Lenght dens.	τ
	ID	(HU)	OBJECTS	(m^3 m^{-3})	(m^3 m^{-3})	(mm^3)	(mm^2)	(x10^6 number m^{-3})	(100%)		(m^3 m^{-3})	(km m^{-3})	
	DU-T	-644	8212	0,110	0,024	13,517	199410,7	1,780	45,8	0,587	376133,673	6,342	0,727
	EL-T	-494	5091	0,096	0,035	31,487	189297,4	1,100	76,6	0,565	290451,550	4,887	1,187
T	ID-T	-524	6297	0,064	0,015	10,076	129774,3	1,360	40,9	0,542	199780,342	4,394	0,860
H	KI-T	-544	6571	0,111	0,021	15,022	188672,5	1,380	72,5	0,679	677864,895	6,185	2,686
1	KO-T	-794	5661	0,081	0,018	14,255	139363,6	1,220	71,2	0,666	362467,917	3,987	1,184
	LA-T	-584	9920	0,098	0,048	22,442	346937,6	2,150	70,7	0,577	941201,849	10,684	1,456
	LI-T	-664	6709	0,094	0,028	19,300	187456,4	1,450	75,6	0,626	460731,212	5,256	1,923
	MO-T	-544	3223	0,061	0,017	24,319	75333,0	0,690	79,1	0,563	74619,368	2,071	0,843
	SD	*97,980*											
	CV%	*23,488*											
	DU-T	-14	30771	0,181	0,089	13,374	809605,9	6,670	82,4	0,666	2464391,383	23,774	12,172
	EL-T	61	8916	0,197	0,070	24,915	413235,3	2,820	84,3	0,600	850964,475	10,856	4,109
T	ID-T	46	13003	0,111	0,022	11,184	188486,8	1,930	43,9	0,559	606065,445	10,832	1,178
H	KI-T	136	12342	0,129	0,069	25,911	552986,0	2,670	89,3	0,667	1842491,014	14,186	10,019
2	KO-T	-309	20513	0,141	0,078	17,638	614459,0	4,440	86,6	0,666	1934680,640	16,752	6,487
	LA-T	1	16275	0,209	0,122	34,558	908260,6	3,530	93,0	0,644	3088460,920	23,494	81,683
	LI-T	36	16637	0,228	0,083	22,924	612609,1	3,600	84,3	0,617	1769390,064	15,777	4,311
	MO-T	-4	10956	0,078	0,031	12,942	200521,1	2,370	67,7	0,577	267892,207	6,137	1,156
	SD	*131,501*											
	CV%	*12,916*											
	DU-T	96	35552	0,327	0,117	30,293	1064785,7	7,712	86,6	0,677	N/A	N/A	N/A
	EL-T	289	16421	0,251	0,097	54,629	620225,7	3,562	87,2	0,633	N/A	N/A	N/A
T	ID-T	309	26168	0,151	0,061	10,736	564330,6	5,676	62,1	0,606	N/A	N/A	N/A
H	KI-T	429	15118	0,143	0,108	32,966	803685,1	3,279	92,2	0,699	N/A	N/A	N/A
3	KO-T	-151	20563	0,142	0,079	17,647	616122,8	4,460	86,7	0,666	N/A	N/A	N/A
	LA-T	236	16276	0,315	0,122	34,558	908261,0	3,531	93,0	0,644	N/A	N/A	N/A
	LI-T	309	20187	0,332	0,174	39,723	1175427,1	4,379	94,4	0,679	N/A	N/A	N/A
	MO-T	269	19819	0,106	0,051	11,884	402770,0	4,299	73,0	0,624	N/A	N/A	N/A
	SD	*177,261*											
	CV%	*14,209*											

N/A: Not available

-Threshold values and detected objects (pores):

Change in the number of the detected pores (Detected Objects) in function of the different threshold values can be seen in Table 3. The increase in detected pores ranges from 64 % (LA-T) to 274 % (DU-T) if we compare the lowest Th_1 to Th_2. While the same increase in volume is changing from 43% (ID-T) to 348% (KO-T). Since the detected amount of pore volume due to the critical role of threshold value is one of the key issues, consistency of the different threshold defining methods needs to be supervised. This practically means that a given voxel intensity can be detected as pore space or soil matrix as well in case two different soil samples. It is necessary to emphasize that there is no computer tomography evaluation protocol, or well-established methods for soil samples. Therefore, the above described procedure and further analysis steps based on my own developed evaluation procedure.

-Macroporosity$_1$:

Macropor$_1$ is derived from the second CT measurement after the long drying section and supposed to represent the total macroporosity ($m^3_{soilair}$ m^{-3}_{soil}). In this state the samples are in one phase, thus the effective macroporosity is approximately equal to the soil total macroporosity. It needs to be emphasised that the results in this study refer to the macroporosity properties solely due to the volume of the smallest pore space being detected (1 voxel = 0,39 x 0,39 x 1,2 mm^3).

-Macroporosity$_2$:

Makropor$_2$ ($m^3_{soilair}$ m^{-3}_{soil}) is connected to the actual state of pore network system at the beginning of the diffusion experiment assuming that no destruction happened during the measurement, thus soils behaved similar in point of water retention (-200 cm matrix potential).

-Mean pore size:

Analyses of mean pore size (mm^{-3}) is well worth considering, as huge crack, high density of root channels or earthworm burrows may have impact on this value.

-Pore surfacearea:

In Table 3. Area represents cumulated value of the voxel surfaces in mm^2. It does not only refer to the overall soil physical properties such as the binding ability of the soil surface, but may also be an interesting indicator for soil surface roughness, which can be linked to habitat of soil microarthropods (Kampichler and Hauser 1993) or fractal parameters, which indicates soil degradation process (Pachepsky et al., 1995).

-Macroporous length density:

Length dens. shows the length density of the macroporous networks in one m^3 soil. Based on these data estimation on water hydraulic conductivity can be drawn (Perret et al. 1999 Koekkoek and Booltink 1999). Since these are derived data, there is a nearly perfect linear regression between these values and the number of pores in all three threshold cases,

-Ratio of pores (with volume > 1000 mm$^)$ in total porosity, POM (100%):

POM (100%) was proposed by Luo et al (2010) and shows the percentage of large pores in total porosity. Without any other studies, high percentage might indicate well-connected pore system, extended internal crack or crush.

-α:

By identification and labelling every single object, accurate pore size data were generated for each soil column. I tested several distribution functions on this dataset (parameter estimation-maximum likelihood method) and found that the Pareto distribution (7) (Grimshaw 1993) gave the best fit, wherein α and x_m are the parameters and they were estimated by the maximum likelihood method. It can be expressed by the following maximum likelihood method, as it can be seen in Figure 6.

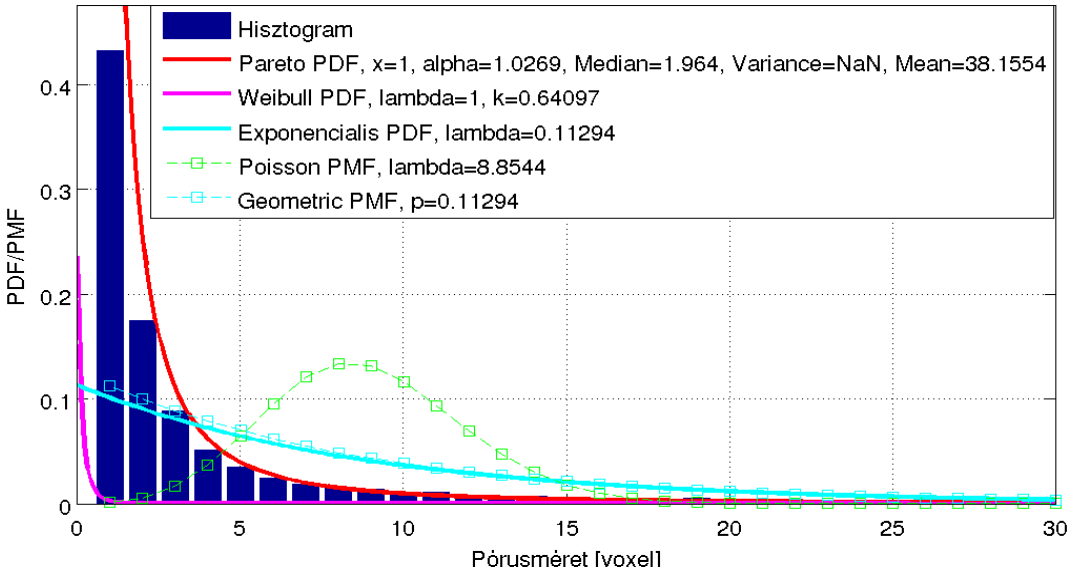

Figure 6.: relevant part of a sample containing 13347 objects. PDF-(probability density function/PMF- probability mass function

$$L(\alpha, x_m) = \prod_{i=1}^{n} \alpha \frac{x_m^{\alpha}}{x_i^{\alpha+1}} = \alpha^n x_m^{n\alpha} \prod_{i=1}^{n} \frac{1}{x_i^{\alpha+1}} \tag{7}$$

$$x_m = \min_i x_i \tag{8}$$

where x_i is the size of the i^{th} pore and therefore x_m is the size of the smallest pore. Values of α were calculated by:

$$\alpha = \frac{n_p}{\sum_{i=1}^{n} (\ln x_i - \ln x_m)}, \tag{9}$$

where n_p is the number of pores. Since x_m is the size of the smallest pore detected which is practically equally to the size of a single voxel, hence this value is constant and identical in all case.

-Length density:

This data show the soil pore length in 1 m^3 soil derived from soil pore skeleton. The average difference between soils is about 9,75 km m^{-3}.

-Node density:

It shows the density of nodes or the number of connections estimated for 1 m^3 soil. The soil pore space connectivity has direct influence on the transport process taking place in soil.

-Tortuosity, τ:

Tortuosity represents the labyrinth factor of the pore structure. It's quite difficult to estimate this parameter, thus there is significant differences in the definitions applied in different research works. In this present study determination of tortuosity was based on pores longer than 100 mm, since pore

skeleton less than 100 mm in length might connected to those pores that are blocked by water film or fall out of the CT detection limit. Therefore this parameter shows the average length of pores longer than 100 mm in length to the length of the soil sample.

Results of the diffusion experiment:

Results of D_g determination:

According to the equation (3). with the help of iteration of the D_g value it became possible to define the best fit, where the sum of square errors was minimal. As the result of this process I obtained the value of diffusion coefficient (D_g) for each gas for every soil sample. For example the value for the MO-T sample is 9 x 10^{-7} m^2 s^{-1}. Then I normalized the obtained gas diffusion value of each soil samples with the diffusion coefficient of the same gas measured at open air at the same pressure and temperature condition to calculate the relative diffusion coefficient representing the gaseous permeability of the given soil sample (Tuli 2002, Lange et al. 2009). I used to following diffusion coefficients (D_0) for CO_2 at open air 1,39 x 10^{-5} m^2 s^{-1} (Gaudinski et al. 2000), for N_2O 1,43 x 10^{-5} m^2 s^{-1} (Pritchard and Currie 1982), 1,7 x 10^{-5} m^2 s^{-1} for CH_4 (Khvorostyanov et al. 2008, von Fischer et al. 2009). Table 4. contains the summary of D_g values for each gas. Because of a system failure during the GC measurement sample ID-T is excluded from further evaluation. The summary of evaluation is presented in table 4.

Table 4.: Diffusion coefficients (D_g) and relative diffusion coefficients (D_g/D_0)

SAMPLE ID	**CO_2**		**N_2O**		**CH_4**	
ID	**D_g**	**D_g/D_0**	**D_g**	**D_g/D_0**	**D_g**	**D_g/D_0**
DU-T	1,4 x10^{-07}	0,0101	2 x10^{-07}	0,0140	2,7 x10^{-07}	0,015864
EL-T	6 x10^{-08}	0,0043	4 x10^{-07}	0,0280	3,1 x10^{-07}	0,018214
ID-T	N/A	N/A	N/A	N/A	N/A	N/A
KI-T	9 x10^{-08}	0,0065	6 x10^{-08}	0,0042	4 x10^{-09}	0,000235
KO-T	1,1 x10^{-08}	0,0008	1,5 x10^{-08}	0,0010	7 x10^{-07}	0,041128
LA-T	5 x10^{-07}	0,0360	3 x10^{-07}	0,0210	8 x10^{-08}	0,0047
LI-T	4 x10^{-08}	0,0029	1,2 x10^{-07}	0,0084	3,1 x10^{-06}	0,182139
MO-T	2 x10^{-07}	0,0144	9 x10^{-07}	0,0629	2,1 x10^{-07}	0,012338

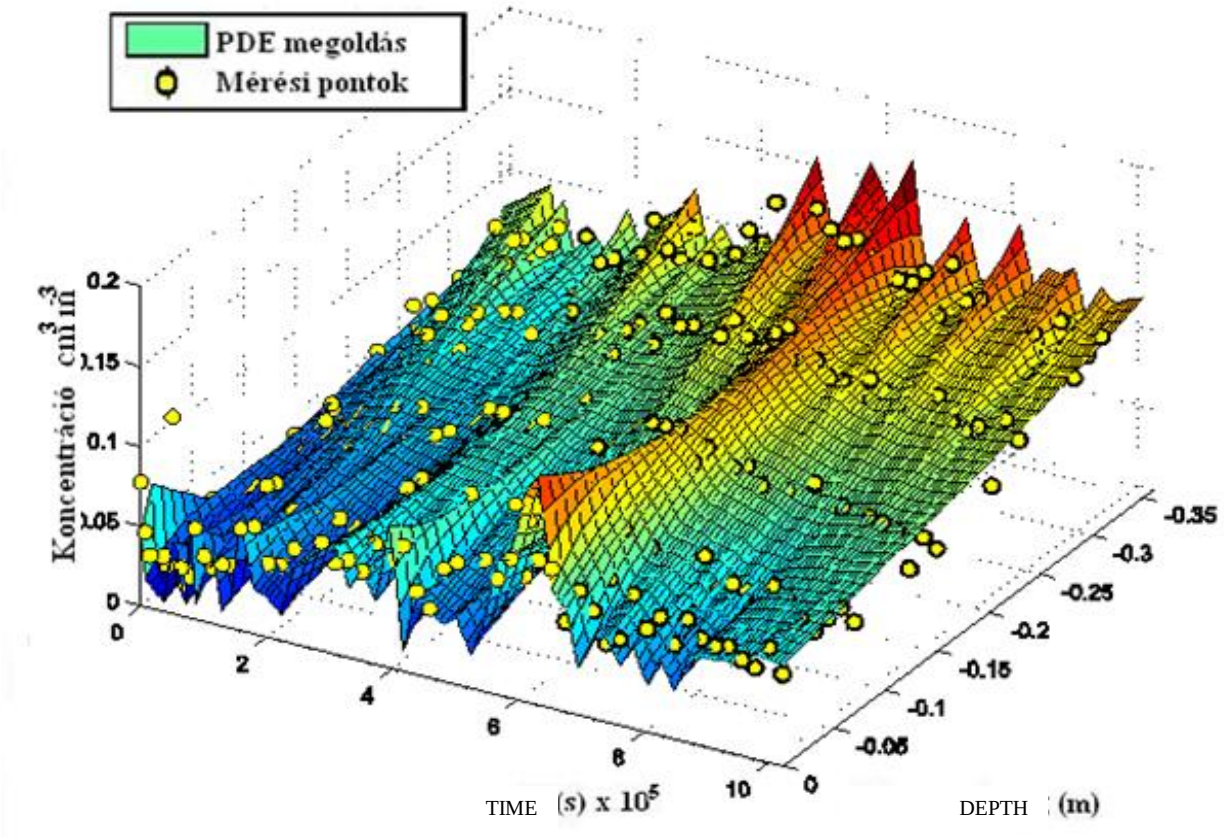

Figure 7.: Results of the numerical modell fitting sample for MO-T in case of carbon dioxide.
D_g= 2 x 10 $^{-07}$ m^2 s^{-1} (Err_A= 1,67%).

Relationship between the relative gas diffusion coefficient and soil parameters:

In this section I connected the results of diffusion experiment (D_g/D_0) to the results of CT data obtained by the three segmentation method and collateral experimental results. My aim was to identify which properties influenced significantly the process of diffusion or to define those soil structure attributes which might help to predict gas permeability of a soil samples.

Multiple linear regression analysis was used, because this method is able to show the effects of several independent variables on one dependent variable. Matrix form was used for prescribing multivariate models (Y, dependent variable, i.e., the relative diffusion coefficient; and X, the independent variable, i.e., soil properties). The parameters of the regression equation for the multivariate model can be determined according to the least squares method.

The standard linear model must be linearly independent (which means linear relationship cannot exists between independent variable, X). If not, multicollinearity occurs. Therefore, I cannot test

together the number of nodes and the detected objects because their relationship is linearly well-defined ($r = 0.851$, $P = 0.015$).
Thus numbers of independent variables were reduced on their connection between other properties.

Based on multiple linear regression analysis the most accurate prediction of relative gas diffusion coefficients was found in the case of independent variables determined by Th_2 threshold regarding all gases. This was proven by the lowest standard error compared to the error results counted by other threshold values. By summarizing the prediction error of the diffusion models per threshold values it can be concluded that the most accurate predictions was found by threshold value Th_1, then by Th_2, which also indicated that the proper segmentation threshold value was between Th_1 and Th_2 for the ongoing experimental work. It is also established that among the soil attributes the amount of pore connection (nodes) was significant independent variable in all but one case. Based on that result I suggested the implementation of this variable for model development describing gaseous diffusion taking place in the porous medium of soil together with the already used ordinary parameters, $macroporosity_1$ and tortuosity, which were also indicated as significant variables by the analysis.

It needs to be emphasized, that these findings are based on very small number of observed cases. (Unfortunately CT measurements are extremely costly.) Therefore, further aim is to test these measurement and evaluation procedures established for the eight large samples with increased amount of soil samples differing in size and physical properties.

Classical one-and two-parameter models for predicting the relative diffusion coefficient:
In the next section I summarised the predictions of the well-known and commonly used classical models estimating relative gaseous diffusion coefficient (Table 5.), where the input values (macroporosity data) were calculated according to the three segmentation methods (Th_1, Th_2, Th_3).

The objectives was to find out which models give a good estimations on the relative gaseous diffusion coefficients of the three measured gases and which threshold determining method provides the most appropriate input parameters. Root mean square error (RMSE) (10) and *bias* (11) were used for model estimation. Root-mean-square deviation (RMSE) was calculated by

$$RMSE = \sqrt{\frac{1}{n}\sum_{i=1}^{n} d_i^2} \qquad (10)$$

and was used to evaluate the average prediction uncertainty in D_g/D_0, where d_i means the difference between the predicted and the measured value, and n is the number of measurements.

Table 5.: Classical one and two parameter models for predicting relative gaseous diffusion coeficient ($\theta_{levegő}$ represents effective porosity, ϕ is the total porosity. In modell PMQ m is 3 for undisturbed and 6 for disturbed soil sample.

Author:	**Name:**	**Model:**
Buckingham 1904	Buckingham	$\frac{D_g}{D_o} = (\theta_{levegő})^2$
Penman 1940	Penman	$\frac{D_g}{D_o} = 0,66\theta_{levegő}$
Van Bavel 1952	Van Bavel	$\frac{D_g}{D_o} = 0,61\theta_{levegő}$
Marshall 1958	Marshall	$\frac{D_g}{D_o} = (\theta_{levegő})^{\frac{3}{2}}$
Grable és Siemer 1968	GS	$\frac{D_g}{D_o} = 10^{-6}\theta_{levegő}^{3,36}$
Lai et al. 1976	Lai	$\frac{D_g}{D_o} = \theta_{levegő}^{\frac{5}{3}}$
Xu et al. 1992	Xu	$\frac{D_g}{D_o} = \frac{(\theta_{levegő})^{2,51}}{\phi^2}$
Millington és Quirk 1960	MQ_1	$\frac{D_g}{D_o} = \frac{(\theta_{levegő})^2}{\phi^{\frac{2}{3}}}$
Millington és Quirk 1961	MQ_2	$\frac{D_g}{D_o} = \frac{(\theta_{levegő})^{\frac{10}{3}}}{\phi^2}$
Moldrup et al. 1997	PQM	$\frac{D_g}{D_0} = 0,66\phi(\frac{\theta_{levegő}}{\phi})^{\frac{12-}{3}^m}$
Moldrup et al. 2005	Moldrup	$\frac{D_g}{D_0} = \phi^2(\frac{\theta_{levegő}}{\phi})^{(2+\frac{\log(\theta_{levegő\,100}^{\frac{1}{4}})}{\log(\frac{\theta_{levegő\,100}}{\phi})}}$

By means of *bias* evaluation of over- or underestimation of the calculated data compared to the measured D_g/D_0 values can be examined:

$$bias = \frac{1}{n}\sum_{i=1}^{n} d_i \qquad (11)$$

The results are presented in Table 6.

Relative diffusion coefficient of carbon dioxide was predicted most accurately among the three gases. Taking into account all model predictions, in case of carbon dioxide and nitrous oxide the Th_1, than Th_2 segmentation methods provided the most accurate input data. Predictions for methane diffusion contradict completely according to the statistical analyses, where porosity values determined by Th_3 segmentation method performed better. So it is important to emphasize again that this review only valid to the present work and more observations are needed to drawn general conclusion on the predictions of the different models.

Table 6.: Statistical analyses of model predictions in function of thresholds

	RMSE/bias	Buckingham	Penman	Van Bavel	Marshall	GS	Lai	XU	MQ_1	MQ_2	PMQ	Moldrup
Th_1	$RMSE_{CO2}$	0,0145	0,0108	0,0100	0,0110	0,0155	0,0128	0,0107	0,0111	0,0139	0,0141	0,0150
	$bias_{CO2}$	-0,0099	0,0073	0,0059	-0,0060	-0,0107	-0,0080	0,0061	-0,0066	-0,0096	-0,0098	-0,0103
	$RMSE_{N2O}$	0,0274	0,0211	0,0211	0,0250	0,0279	0,0262	0,0236	0,0253	0,0272	0,0273	0,0277
	$bias_{N2O}$	-0,0191	-0,0020	-0,0033	-0,0152	-0,0199	-0,0173	-0,0031	-0,0159	-0,0188	-0,0191	-0,0196
	$RMSE_{CH4}$	0,0709	0,0639	0,0643	0,0691	0,0713	0,0701	0,0673	0,0695	0,0709	0,0711	0,0712
	$bias_{CH4}$	-0,0384	-0,0213	-0,0226	-0,0345	-0,0392	-0,0366	-0,0224	-0,0352	-0,0381	-0,0384	-0,0389
		Buckingham	**Penman**	**Van Bavel**	**Marshall**	**GS**	**Lai**	**XU**	**MQ_1**	**MQ_2**	**PMQ**	**Moldrup**
Th_2	$RMSE_{CO2}$	0,0098	0,0431	0,0391	0,0153	0,0155	0,0097	0,0585	0,0138	0,0084	0,0096	0,0119
	$bias_{CO2}$	-0,0040	0,0405	0,0366	0,0118	-0,0107	0,0042	0,0526	0,0103	-0,0023	-0,0042	-0,0071
	$RMSE_{N2O}$	0,0253	0,0450	0,0415	0,0265	0,0279	0,0246	0,0615	0,0264	0,0253	0,0258	0,0263
	$bias_{N2O}$	-0,0133	0,0313	0,0274	0,0025	-0,0199	-0,0050	0,0433	0,0011	-0,0115	-0,0135	-0,0163
	$RMSE_{CH4}$	0,0681	0,0620	0,0611	0,0625	0,0713	0,0647	0,0796	0,0644	0,0688	0,0696	0,0695
	$bias_{CH4}$	-0,0326	0,0120	0,0081	-0,0168	-0,0392	-0,0243	0,0240	-0,0182	-0,0308	-0,0328	-0,0356
		Buckingham	**Penman**	**Van Bavel**	**Marshall**	**GS**	**Lai**	**XU**	**MQ_1**	**MQ_2**	**PMQ**	**Moldrup**
Th_3	$RMSE_{CO2}$	0,0143	0,0652	0,0597	0,0333	0,0155	0,0234	0,0886	0,0297	0,0170	0,0168	0,0131
	$bias_{CO2}$	0,0020	0,0598	0,0545	0,0257	-0,0107	0,0148	0,0710	0,0215	0,0027	-0,0004	-0,0032
	$RMSE_{N2O}$	0,0256	0,0634	0,0582	0,0365	0,0279	0,0296	0,0865	0,0337	0,0271	0,0275	0,0257
	$bias_{N2O}$	-0,0073	0,0506	0,0452	0,0164	-0,0199	0,0056	0,0618	0,0122	-0,0065	-0,0096	-0,0124
	$RMSE_{CH4}$	0,0594	0,0558	0,0536	0,0475	0,0713	0,0514	0,0808	0,0497	0,0612	0,0653	0,0636
	$bias_{CH4}$	-0,0266	0,0313	0,0259	-0,0029	-0,0392	-0,0137	0,0425	-0,0071	-0,0258	-0,0289	-0,0317

-Model development:

The PMQ model belongs to the most commonly used model due to its accurate estimation on relative diffusion coefficient. In this work it is also confirmed on the basis of RMSE values compared to the other models. As its name shows, this model consists of two models. The model MQ (Moldrup et al. 1997) has a structure dependent variable *m* standing for tortuosity, which value is 3 for undisturbed soils and 6 for soils with repacked or disturbed structure. In the case of sifting or disturbing the original structure the natural macroporous system will be either damaged or eliminated, thus the remaining pore structure is originating from pore space between the sifted soil particles, which should be more tortuous than the original structure. On the basis of this, I proposed modification of the original value *m=3* of PMQ model to 6. Value 0,66, in Penman model representing also tortuosity, makes the model inflexible. Therefore, I suggest replacing this value by parameter α calculated and presented based on the Pareto distribution (9).

-Results of the proposed model:

Through these modifications loss of rigidity from the Penman model can be seen as application of parameter α ensures that a pore space characteristics parameter of each soil samples is involved instead of universal constants. Therefore model prediction quality is improved compared to the original PMQ model.

The RMSE and *bias* of the model estimations listed in Table 7.

Table 7.: Statistical evaluation of the model proposed

Th_1	**$RMSE_{CO2}$**	0,0129	**Th_2**	**$RMSE_{CO2}$**	0,0088	**Th_3**	**$RMSE_{CO2}$**	0,0211
	$bias_{CO2}$	-0,0088		**$bias_{CO2}$**	0,0015		**$bias_{CO2}$**	0,0079
	$RMSE_{N2O}$	0,0266		**$RMSE_{N2O}$**	0,0253		**$RMSE_{N2O}$**	0,0290
	$bias_{N2O}$	-0,0180		**$bias_{N2O}$**	-0,0077		**$bias_{N2O}$**	-0,0013
	$RMSE_{CH4}$	0,0706		**$RMSE_{CH4}$**	0,0679		**$RMSE_{CH4}$**	0,0598
	$bias_{CH4}$	-0,0373		**$bias_{CH4}$**	-0,0270		**$bias_{CH4}$**	-0,0206

The proposed model with the input data from Th_2 segmentation method was the best among the two parameter models and it gave the second best prediction taking into account all models. Based on these results I declared these modifications efficient and recommend more extent model testing.

Table 8.: Summarized RMSE of the three gases in the case of Th_2 segmentation method

NÉV	**Buck.**	**Penm.**	**Van B.**	**Marsh.**	**GS**	**Lai**	**XU**	**MQ_1**	**MQ_2**	**PMQ**	**Moldr.**	**Javasolt**
$RMSE_\Sigma$	0,103	0,150	0,142	0,104	0,115	0,099	0,199	0,105	0,103	0,105	0,108	0,102
PARAMÉTEREK SZÁMA	1	1	1	1	1	1	2	2	2	2	2	2

NEW RESULTS

Based on the experimental examination of soil gaseous diffusion and computed tomography analyses of the soil pore structure I achieved the following new results:

- In this work I presented a new experimental setup, which enables us to follow the concentration change caused by gaseous diffusion in case of undisturbed and disturbed soil samples. Analyses of soil pore space and structure properties (which previous determination was very difficult or impossible, e.g.: 3D pore connectivity) became available in function of the relative diffusion coefficient due to successful combination of gas diffusion experiment with modern computed tomography.
- Based on multiple linear regression analysis the most accurate prediction of relative gas diffusion coefficients was found in the case of independent variables determined by Th_2 threshold regarding all gases. This was proven by the lowest standard error compared to the error results counted by other threshold values. By summarizing the prediction error of the diffusion models per threshold values it can be concluded that the most accurate predictions was found by threshold value Th_1, then by Th_2, which also indicated that the proper segmentation threshold value was between Th_1 and Th_2 for the ongoing experimental work.

- It is also established that among the soil attributes the amount of pore connection (nodes) was significant independent variable in all but one case. Based on that result I suggested the implementation of this variable for model development describing gaseous diffusion taking place in the porous medium of soil together with the already used ordinary parameters, $macroporosity_1$ and tortuosity, which were also indicated as significant variables by the analysis.

- Evaluating the summarized performance of all tested models the Buckingham (Buckingham 1904), Lai (Lai et al. 1976) and MQ_2 models (Millington and Quirk 1961) produced the best results. As the result of this investigation I suggested two modifications of the widely used PMQ model (Moldrup et al. 1997) by changing the multiplier from Penman model to the parameter which based on maximum likelihood estimation function of the Pareto distribution. It dissolved the inflexibility of the PMQ model. Second recommendation was

the change of the structure dependant *m* parameter representing the tortuosity from 3 to 6 for soil with intact structure. Comparing the prediction errors of the new model with the original PMQ model's I found that from 7 out of 9 cases it performed more accurately. Beside this, the proposed model with the input data from Th_2 segmentation method was the best among the two parameter models and it gave the second best prediction taking into account all models. Based on these results and I declared these modifications efficient and recommended more extended model testing.

- The theoretical study of convective transport processes is closely related to the presented work. Our outstanding results are published in Journal of Physics A: Mathematical and Theoretical (2007, 40, 1-9 p.).

- Finally, practical applicability needs to be emphasized, in which theoretical and practical aspects are defined currently as the further steps of this research work:
    - There is an opportunity to test experimentally the novel application of Riccati ordinary differential equations proposed in Mészáros et al. 2011.
    - On the basis of experimental system soil structure database can be created by diverse samples classified by soil genetic or texture.

RECOMMENDATIONS

Based on the achieved results I recommend the followings in order to develop the quality of this work and to connect the results with other studies:

Recommendations for extending the present experimental settings:

- The most restrictive factor of the present work is the small number of observations. By reason of this, general conclusion cannot be drawn. Therefore, the next goal of my work is to increase the number of the soil samples involved in the diffusion experiments and computer tomography examination, where the sample size, texture and water content cover wider spectrum.

- I propose extension of the experimental equipment with magnetic resonance imaging (MRI), which can separate soil and water filled voxels. So MRI enables to prevent structure change in soil pore system during the drying phase if samples can be scanned immediately before and after the diffusion experiment.

- I consider depth as a very important factor to test, thus revealing the connection between relative diffusion coefficient and porosity in function of depth would help us to determine the optimal sample size, which can describe the soil gaseous permeability. Taking into account the economics reasons adequate sample size for characterization of large areas might significantly reduced the releases.

- I recommend linking soil pore space skeleton, determined by computer tomography evaluation, to the pore size at nodes (connecting voxels), which could be utilized as a skeleton model able to simulate the formation of dead zones by different levels of saturation.

- I highly recommend elaborating standardized CT segmentation and data evaluation process for soil samples (with different texture and saturation) similarly to medical practice.

Suggestions and drafts for theoretical and experimental research of complex liquid and gas phased coupled transport procedures:

- In the presented work examination of soil gas transport was limited to diffusion, however it is related to two main transport processes under natural condition: convection and diffusion. In the presented experimental setup there was no macroscopic convective flow generated due to the low temperature gradient, but this does not allow us to threat these phenomena separately (Kirchner et al. 2006). If temperature gradient occures in soil or in the air above the soil surface that becomes driving force for mixing the gaseous phase with higher kinetic energy, thereby heat transfer occurs. Convective flow generates spectacular natural phenomena: for example frost pattern means the naturally occurring round, strip or polygon shaped layer of the top soil, where the classic Rayleigh–Bènard flow pattern can be observed (Gyarmati 2005, Mészáros et al. 2007). With the help of an infrared camera convective heat flows generated on the soil-atmosphere interface are perfectly observable (Vitál et al. 2007, Nagy et al. 2011). In relation with this, as a result of our previous research a theoretic model is elaborated (Gyarmati 2005, Mészáros et al. 2007, Kirschner et al. 2007) to describe convective instabilities and (Gyarmati et al. 2007) transports in cylindrical systems, in which the description of the velocity function is based on the Ostroumov-problem (Osrtoumov 1958). Fourth order ordinary differential equation describing radial dependence of velocity was solved directly by a mathematic program package able to perform symbolic calculations. The resulted velocity function is in good accordance with the previous simulation results (Kirschner et al. 2007, Gyarmati et al. 2007). However the experimental validation of this model has not been done yet. According to this I recommend the repeat of the diffusion experiment with adjustment assisting to the generation of convective flows; the repeated measurement provides the opportunity to examine the validity of the theoretic model.

- I also planned to combine these results with my previous nitrogen transformation reaction kinetic experiments (Gyarmati et al. 2011, Hárshegyi et al. 2008). Moreover – in case of opportunity – I would like to test the relationship between heavy metal mobility and soil structure with and without vegetation (Bálint et al. 2007, Gyarmati et al. 2008, Bernvalner et al. 2011).

References:

BÁLINT, Á., GYARMATI, B., FODOR, I., KISS, R. (2007): Examination of several heavy metals in plants and soil of a shelter-belt, *Cereal Research Communications*, 35 (2) 193-196. p.

BERNVALNER, G., GYARMATI, B., TÖRŐ, B., ERDŐSI, K.,BÁLINT, Á. (2011): Investigation of the effect of zinc and copper on Lepidium Sativum in pot experiment, *Növénytermelés*, 60, 223-226. p.

BLAKE, G.R., HARTGE, K.H. (1986): Bulk Density. In: KLUTE, A. (Szerk) *Methods of Soil Analysis, Part I. Physical and Mineralogical Methods: Agronomy Monograph no. 9*, Madison, WI: 2nd edn. Am Soc Agron, 363-375. p.

BUCKINGHAM, E. (1904): Contributions to our knowledge of the aeration of soils. *Bulletin 25. U.S. Department of Agriculture Bureau of Soils*, Washington DC

CAPOWIEZ, Y., PIERRET, A., DANIEL, O., MONESTIEZ, P. (1998): 3D skeleton reconstruction of natural earthworm burrow systems using CAT scan images of soil cores. *Biology and Fertility of Soils*, 27, 51-59. p.

E DIN ISO 11277:1994 Bodenbeschaffenheit. Bestimmung der Partikelgrößenverteilung in Mineralböden. Verfahren durch Sieben und Sedimentation nach Entfernen der löslichen Salze der organischen Substanz und der Carbonate. Beuth-Verlag, Berlin

GAUDINSKY, J.B., TRUMBORE, S.E., DAVIDSON, E.A., ZHENG, S.H. (2000): Soil carbon cycling in a temperate forest: Radiocarbon based estimates of residence times, sequestration rates and partitioning of fluxes. *Biogeochemistry*, 51 (1) 33-69. p. doi: 10.l023/A:1006301010014

GRABLE, A.R., SIEMER, E. G. (1968): Effects of Bulk Density, Aggregate Size, and Soil Water Suction on Oxygen Diffusion, Redox Potentials, and Elongation of Corn Roots, *Soil Science Society of America Journal*, 32 (2) 180-186. p.

GRIMSHAW, S.D. (1993): Computing maximum likelihood estimates for generalized Pareto distribution. *Technometrics*, 35, 185-191. p.

HARSHEGYI, Z., GYARMATI, B., HELTAI, G., MESZAROS, C., BALINT, A. (2008): Modelling with kinetic equations of transformation of different nitrogen fertilizer in a soil core incubation and a pot experiment. *Cereal Research Communications* 36 (3) 1679-1682. p.

HOUNSFIELD, G. N. (1973): Computerized transverse axial scanning (tomography): Description of system. *British Journal of Radiology*, 46 (552) 1016-1022. p.

KAMPICHLER, C., HAUSER, M. (1993): Roughness of soil pore surface and its effect on available habitat space of microarthropods, *Geoderma*, 56, 223-232. p.

KHVOROSTYANOV, D. V., CIAIS, P., KRINNER, G., ZIMOV, S.A. (2008): Vulnerability of east Siberia's frozen carbon stores to future warming, *Geophysical Research Letters*, 35, 5. p. L10703, doi: 10.1029/2008GL033639.

KIRSCHNER, I, BÁLINT, Á., CSIKJA, R., GYARMATI, B., BALOGH, A., MÉSZÁROS, CS. (2007): An approximate symbolic solution for convective instability flows in vertical cylindrical tubes, *J. Phys. A: Math. Theor*. 40, 1-9. p.

KOEKKOEK, E.J.W., BOOLTINK, H. (1999): Neural network models to predict soil water retention *European Journal of Soil Science*, 50 (3) 489–495.p.

LAI, S., TIEDJE J.M., ERICKSON. A.E. (1976): In situ measurement of gas diffusion coefficient in soils. *Soil Science Society of America Journal*, 40, 3–6. p.

LANGE, S. F., ALLAIRE, S. E., ROLSTON, D. E. (2009): Soil-gas diffusivity in large soil monoliths. *European Journal of Soil Science*, 60, 1065-1077. p.

LIU, G., LI, B., HU, K., VAN GENUCHTEN, M.TH. (2006): Simulating the gas diffusion coefficient in macropore network images: influence of soil pore morphology, *Soil Science Society of America Journal*, 70, 1252-1261. p.

LUO, L., LIN, H., LI, S. (2010): Quantification of 3 D soil macropore networks in different types and land uses using computed tomography. *Journal of Hydrology*, 393, 53-64. p.

MARSHALL, T. J. (1958): A relation between permeability and size distribution of pores. *Journal of Soil Science*, 9, 1-8. p.

MathWorks-ref1, www.mathworks.com/help/techdoc/ref/pdepe.html

MathWorks-ref2, www.mathworks.com/help/techdoc/ref/fminsearch.html

MEIJERING, E.H.W., NIESSEN, W.J., PLUIM, J.P.W., VIERGEVER, M.A. (1999): Quantitative comparison of sinc-approximating kernels for medical image interpolation in medical image computing and computer-assisted intervention In: TAYLOR, C., COLCHESTER, A. (Szerk.), *vol. 1679 of Lecture Notes in Computer Science, MICCAI 1999.*, Berlin: Springer-Verlag, 210-217. p.

MÉSZÁROS, CS., GOTTSCHALK, K., FARKAS, I., GYARMATI, B., BÁLINT, Á. (2011): Surface Waves at Convection-diffusion Processes through Porous Media, *Mechanical Engineering Letters: R&D: Research & Development* 6, 95-102 p.

MÉSZÁROS, CS., GOTTSCHALK, K., JESZENŐI, G., GYARMATI, B., FÖLDI, A.,BÁLINT, Á. (2008): Transient character of transport processes in binary mixtures In: Farkas I (szerk.), 14th Workshop on Energy and Environment: Book of Abstracts. Konferencia helye, ideje: Gödöllő, Magyarország

MÉSZÁROS, CS., GYARMATI, B., BÁLINT, Á. (2007): Asymptotic Solution for Convective Instability Flows in Vertical Cylindrical Tubes, In: Conference of Research and Teaching of Physics in the Context of University Education, Nitra, Szlovákia, (ISBN:978-80-8069.898-0) Slovak Agricultural University, 49-52 p.

MÉSZÁROS, CS., KIRSCHNER, I., GOTTSCHALK, K., SZÉKELY, L., BÁLINT, Á. (2010): Symbolic solutions of ordinary differential equation systems used for coupled transport processes,
Mechanical Engineering Letters: R&D: Research & Development 4, 121-140 p.

MÉSZÁROS, CS., GYARMATI, B., BÁLINT, Á. (2007): Asymptotic Solution for Convective Instability Flows in Vertical Cylindrical Tubes In: Conference of Research and Teaching of Physics in the Context of University Education, (ISBN:978-80-8069.898-0) Slovak Agricultural University 49-52 p.

MILLINGTON, R. J., QUIRK, J. P. (1959): Permeability of porous media. *Nature*, 183, 387-388. p.

MILLINGTON, R.J., QUIRK, J.M. (1960): Transport in porous media. In: VAN BUREN, F.A. et al. (Szerk.) *Transactions of the International Congress of Soil Science, 7th, Madison, WI*, Amsterdam: Elsevier, 97-106. p.

MILLINGTON, R.J., QUIRK, J.M. (1961): Permeability of porous solids. *Transactions of the Faraday Society*, 57, 1200-1207. p.

MOLDRUP, P., OLESEN, T., ROLSTON, D.E., YAMAGUCHI, T. (1997): Modelling diffusion and reaction in soils: VII. Predicting gas and ion diffusivity in undisturbed and sieved soils. *Soil Science*, 162, 632-640. p.

NAGY, N., GYARMATI, B., MÉSZÁROS, CS., GOTTSCHALK, K., BÁLINT, Á. (2011): Konvekció hengeres talaj rendszerekben, In: Bodnár Ákos (szerk.),Tehetségnap, SZIE MKK Tudományos Diákköri Rendezvény, Gödöllő, Magyarország, (ISBN:978-963-269-235-7) Gödöllő: Szent István Egyetem, 26-29 p.

NAGY, N., GYARMATI, B., MÉSZÁROS, CS., GOTTSCHALK, K., BÁLINT, Á. (2011): Konvekció hengeres talaj rendszerekben *GÉP* LXII.**:** (6.) *36-40.* p.

OSTROUMOV, G. A. (1958): Free convection under the conditions of internal problem. *NACA Technical memorandum*, 1407 p.

PACHEPSKY, Y.A., POLUBESOVA, T. A., HAJNOS, M., SOKOLOWSKA, Z., JÓZEFACIUK, Z. (1995): Fractal Parameters of Pore Surface Area as Influenced by Simulated Soil *Degradation Soil Science Society of America Journal*, 59 (1) 68-75. p.

PENMAN, H. L. (1940): Gas and vapor movements in the soil. I. The diffusion of vapours through porous solids. *The Journal of Agricultural Science*, 30, 437-462. p.

PERRET, J., PRASHER, S.O., KANTZAS, A., LANGFORD, C. (1999): Three-dimensional quantification of macropore networks in undisturbed soil cores. *Soil Science Society of America Journal*, 63, 1530-1543. p.

PRITCHARD, D.T., CURRIE, J.A. (1982): Diffusion coefficients of carbon dioxide, nitrous oxide, ethylene and ethane in air and their measurement. *Journal of Soil Science*, 33, 175-184. p.

SATO, M., BITTER, I., BENDER, M.A., KAUFMAN, A.E., NAKAJIMA, M. (2000): TEASAR: tree-structure extraction algorithm for accurate and robust skeletons. *Proceedings of The Eighth Pacific Conference on Computer Graphics and Applications*, 281, 449. p.

SCHUMACHER, B.A. (2002): Methods for the determination of total organic carbon (TOC) in soils and sediments. NCEA-C- 1282 EMASC-001 online elérhető: http://epa.gov/nerlesd1/cmb/research/papers/bs116.pdf

TARQUIS, A.M., HECK, R.J., GRAU, J.B., FABREGAT, J., SANCHEZ, M.E., ANTÓN, J.M. (2008): Influence of thresholding in mass and entropy dimension of 3-D soil images. *Nonlinear Processes in Geophysics*, 15, 881-891.p. doi:10.5194/npg-15-881-2008

TULI, A. (2002): PHD thesis: Pore geometry effect on gaseous diffusion and convective fluid flow in soils. University of California at Davis, Dept. of Land, Air and Water Resources, U.S.A.

VAN BAVEL, C.H.M. (1952): Gaseous diffusion and porosity in porous media. *Soil Science* 73, 91–104. p.

VITÁL, V., GYARMATI, B., BÁLINT, Á., MÉSZÁROS, CS. (2007): Stacionáriusan körüláramlott gömb alakú szilárd test felületi hőmérsékletváltozásai, Tóth L, Magó L (szerk.) Magyar Tudományos Akadémia Agrártudományok Osztálya Agrárműszaki Bizottság Kutatási és Fejlesztési Tanácskozás Nr. 31, FVM Mezőgazdasági Gépesítési Intézet, (ISBN:978 963 611 4465)
128-132 p.

VON FISCHER, J.C., BUTTERS, G., DUCHATEAU, P.C., THELWELL, P.J., SILLER, R. (2009): In situ measures of methanotroph activity in upland soils: A reactiondiffusion model and field observation of water stress, *Journal of Geophysical Research*, 114 G01015, doi:10.1029/2008JG000731,

WELLER, U., IPPISCH, O., KÖHNE, M., VOGEL, H.J. (2011): Direct Measurement of Unsaturated Conductivity including Hydraulic Nonequilibrium and Hysteresis. *Vadose Zone Journal*, 10 (2) 654-661. p.

XU, X., NIEBER, J.L., GUPTA, S.C. (1992): Compaction effect on the gas diffusion coefficient on soils. *Soil Science Society of America Journal*, 56 1743-1750. p.

PUBLICATIONS RELATED TO TOPIC OF THE DISSERTATION

Publications related to the topic of the dissertation (transport processes, diffusion, convection, modelling, soil examinations, greenhause gases)**:**

Scientific articles published in foreign language:

KIRSCHNER, I, BÁLINT, Á., CSIKJA, R., **GYARMATI, B**., BALOGH, A., MÉSZÁROS, CS. (2007): An approximate symbolic solution for convective instability flows in vertical cylindrical tubes, *J. Phys. A: Math. Theor*. 40, 1-9. p.

GOTTSCHALK, K., MÉSZÁROS, CS., FÖLDI, A., **GYARMATI, B**., FARKAS, I., BÁLINT, Á. (2008): Transient Character of Transport Processes in Binary Mixtures, *Mechanical Engineering Letters* : *R&D : Research & Development*, 1, 200-212. p

MÉSZÁROS, CS., GOTTSCHALK, K., FARKAS, I., **GYARMATI, B**., BÁLINT, Á. (2011): Surface Waves at Convection-diffusion Processes through Porous Media, *Mechanical Engineering Letters: R&D: Research & Development* 6, 95-102 p.

Scientific articles published in Hungarian language:

GYARMATI, B., HÁRSHEGYI, ZS., HELTAI, GY., MÉSZÁROS, CS., BÁLINT Á. (2011): Inkubációs talajoszlop kísérlet nitrogén transzformációs folyamatainak reakciókinetikai modellezése, *Agrokémia és Talajtan*, 60 (1) 119-131. p.

NAGY, N., **GYARMATI, B**., MÉSZÁROS, CS., GOTTSCHALK, K., BÁLINT, Á. (2011): Konvekció hengeres talaj rendszerekben *GÉP* LXII.**:** (6.) *36-40.* p.

Conference proceeding in foreign language (full text):

KIRSCHNER, I., BÁLINT, Á., MÉSZÁROS, CS., GOTTSCHALK, K., **GYARMATI, B**., FARKAS, I. (2006): Percolation and fractal models in coupled heat and mass transfer through porous media, In: Farkas I (szerk.) *Drying 2006 Vol A-C. Proceedings of the 15th International Symposium*, Budapest, Magyarország, 163-168 p.

MÉSZÁROS, CS., **GYARMATI, B**., BÁLINT, Á. (2007): Asymptotic Solution for Convective Instability Flows in Vertical Cylindrical Tubes, In: Conference of Research and Teaching of Physics in the Context of University Education, Nitra, Szlovákia, (ISBN:978-80-8069.898-0) Slovak Agricultural University, 49-52 p.

HARSHEGYI, Z., **GYARMATI, B**., HELTAI, G., MESZAROS, C., BALINT, A. (2008): Modelling with kinetic equations of transformation of different nitrogen fertilizer in a soil core incubation and a pot experiment. *Cereal Research Communications* 36 (3) 1679-1682. p.

GYARMATI, B., MÉSZÁROS, CS., HÁRSHEGYI, ZS., KAMPFL, GY, BÁLINT, A. (2008): Effect of different nitrogen fertilizer on physiological parameters of garden cress (*Lepidium sativum*), *Cereal Research Communications*, 36 (3, Suppl. 5) 1683-1686 p.

Conference proceeding in Hungarian language (full text):

MÉSZÁROS, CS., BÁLINT, Á., VITÁL, V., **GYARMATI, B**. (2007): Stacionáriusan körüláramlott gömb alakú szilárd test felületi hőmérsékletváltozásai (Surface temperature changes of the spherical solid body surrounded by stationary flow), XXXI. Kutatási és Fejlesztési Tanácskozás (31st Conference on research and development in agricultural engineering) Nr. 31. 2. kötet. Edited: Dr. Tóth László és Dr. Magó László. Felelős kiadó: (Eds.) Dr. Fenyvesi László. Készült: SZIE, Gödöllő. Magyarország. 128-132 p.

NAGY, N., **GYARMATI, B.**, MÉSZÁROS, CS., GOTTSCHALK, K., BÁLINT, Á. (2011): Talajoszlopok száradásának vizsgálata infravörös sugárzás hatására In: Víg P (szerk.) 7. Magyar Szárítási Szimpózium Gödöllő, Szent István Egyetem, 1-9 p .(ISBN:978-963-269-211-1)

Conference abstracts:

GYARMATI, B., KAMPFL, GY., KUSLITS, M., FÖLDES, T., STANGE, C.F., BÁLINT, Á. (2010): Study on vertical distribution of N_2O and SF_6 gases in quasi-undisturbed soil, Farkas I (szerk.) 16th Workshop on Energy and Environment: Book of Abstracts, Gödöllő, Magyarország 13 p.

GYARMATI, B., BÁLINT, Á., GOTTSCHALK, K., FARKAS, I., MÉSZÁROS, CS. (2007): An analytical solution for convective instability flows in verical cylindrical tubes, Book of abstract,13th Workshop on Energy and Environment, Gödöllő, Magyarország, 19 p.

NAGY, N., MÉSZÁROS, CS., GOTTSCHALK, K., **GYARMATI**, B., BÁLINT, Á. (2010): Convection in cylindrical soil systems, Book of abstract , 16th Workshop on Energy and Environment, Gödöllő, Magyarország, 14 p.

Part of book:

BÁLINT, Á., KAMPFL, GY., NÓTÁS, E., HOFFMANN, S., BERECZ, K., KRISTÓF, K., ANTON, A., SZILI-KOVÁCS, T., **GYARMATI, B**., HELTAI GY., (2010): Az üvegházhatású nitrogén oxidok és széndioxid képződése a talajban. In: LUKÁCS, G. (szerk.) A konferencia előadásainak összefoglalói: 52nd Georgikon Scientific Conferenc Abstracts: Keszthely: Pannon Agrártudományi Egyetem Georgikon Mezőgazdaságtudományi Kar, 1-10. p. (ISBN:978-963-9639-38-6, 978-963-9639-39-3)

BÁLINT, Á., HOFFMANN, S., BERECZ, K., KRISTÓF, K., KAMPFL, GY., NÓTÁS, E., HORVÁTH, M., **GYARMATI, B**., MOLNÁR, E., ANTON, A., SZILI-KOVÁCS, T., HELTAI, GY. (2012): Influence of fertilisation practice on gas and grain yield production In: Richards KG, Fenton O, Watson CJ (szerk.) 17th International Nitrogen Workshop, Ireland, Wexford: Teagasc The National Food Centre, 126-127.p. (ISBN:978-1-84170-588-0, 1-84170-588-8)